Vol. 77, No. 10

Ribavirin Treatment Up-Regulates Antiviral Gene Expression via the Interferon-Stimulated Response Element in Respiratory Syncytial Virus-Infected Epithelial Cells

Yuhong Zhang,[1] Mohammad Jamaluddin,[1] Shaofei Wang,[1] Bing Tian,[1]
Roberto P. Garofalo,[2,3] Antonella Casola,[2] and Allan R. Brasier[1,4]*

*Departments of Medicine,[1] Pediatrics,[2] and Microbiology and Immunology,[3] and Sealy Center for Molecular
Sciences,[4] The University of Texas Medical Branch, Galveston, Texas 77555-1060*

Respiratory syncytial virus (RSV) is a mucosa-restricted virus that is a leading cause of epidemic respiratory tract infections in children. RSV replication is a potent activator of the epithelial-cell genomic response, influencing the expression of a spectrum of cellular pathways, including proinflammatory chemokines of the CC, CXC, and CX$_3$C subclasses. Ribavirin (1-β-D-ribofuranosyl-1,2,4-triazole-3-carboxamide) is a nontoxic antiviral agent currently licensed for the treatment of severe RSV lower respiratory tract infections. Because ribavirin treatment reduces the cytopathic effect in infected cells, we used high-density microarrays to investigate the hypothesis that ribavirin modifies the virus-induced epithelial genomic response to replicating virus. Ribavirin treatment administered in concentrations of 10 to 100 μg/ml potently inhibited RSV transcription, thereby reducing the level of RSV N transcripts to ~13% of levels in nontreated cells. We observed that in both the absence and the presence of ribavirin, RSV infection induced global alterations in the host epithelial cell, affecting ~49% of the ~6,650 expressed genes detectable by the microarray. Ribavirin influences the expression of only 7.5% of the RSV-inducible genes (total number of genes, 272), suggesting that the epithelial-cell genetic program initiated by viral infection is independent of high-level RSV replication. Hierarchical clustering of the ribavirin-regulated genes identified four expression patterns. In one group, ribavirin inhibited the expression of the RSV-inducible CC chemokines MIP-1α and -1β, which are important in RSV-induced pulmonary pathology, and interferon (IFN), a cytokine important in the mucosal immune response. In a second group, ribavirin further up-regulated a set of RSV- and IFN-stimulated response genes (ISGs) encoding antiviral proteins (MxA and p56), complement products, acute-phase response factors, and the STAT and IRF transcription factors. Because IFN-β expression itself was reduced in the ribavirin-treated cells, we further investigated the mechanism for up-regulation of the IFN-signaling pathway. Enhanced expression of IFI 6-16, IFI 9-27, MxA/p78, STAT-1α, STAT-1β, IRF-7B, and TAP-1–LMP2 transcripts were independently reproduced by Northern blot analysis. Ribavirin-enhanced TAP-1–LMP2 expression was a transcriptional event where site mutations of the IFN-stimulated response element (ISRE) blocked RSV and ribavirin-inducible promoter activity. Furthermore, ribavirin up-regulated the transcriptional activity of a reporter gene selectively driven by the ISRE. In specific DNA pull-down assays, we observed that ribavirin enhanced RSV-induced STAT-1 binding to the ISRE. We conclude that ribavirin potentiates virus-induced ISRE signaling to enhance the expression of antiviral ISGs, suggesting a mechanism for the efficacy of combined treatment with ribavirin and IFN in other chronic viral diseases.

Respiratory syncytial virus (RSV) is a nonsegmented negative-strand RNA virus that is the primary etiologic agent of lower respiratory tract (LRT) infections in infants and young children (31). In the United States, almost all children by the age of 3 years will have been infected by RSV (27); in the first 3 years of life, this initial infection will typically be the most severe and likely to produce LRT infection (32, 53, 65). It is estimated that ~4.3 million children in underdeveloped countries die annually from LRT infections (22). Moreover, RSV-induced LRT infections are an increasing cause of morbidity as the proportion of hospitalizations associated with bronchiolitis in infants has risen from 22 to 47% from 1980 to 1996 (53). In fact, over 70% of children with RSV LRT infections experi-

ence impaired pulmonary function for up to 10 years afterwards (42). Based on its ability to produce LRT infections in infants, its induction of recurrent wheezing in children with established atopy, and its high mortality rate for children with underlying pulmonary or cardiac diseases, RSV remains a significant health problem worldwide (32, 43, 54, 65).

In natural infections, RSV replicates primarily in the airway epithelium, producing epithelial damage (2) and perivascular mononuclear infiltration (19). Because the epithelium is now recognized to be an important site for the initiation and coordination of pulmonary inflammation (1), the molecular biology of RSV replication and the virus's ability to induce epithelial-cell signaling have been intensively investigated. After its adsorption to the cell surface, a process taking several hours in vitro (6), the 10 major viral proteins are produced in the cytoplasm by transcription, with the antisense genome being used as a template through a sequential stop-start mechanism that is dependent on viral-RNA-dependent RNA polymerase

L (29, 66). Reverse genetic studies have shown that RSV L is essential for viral mRNA transcription as well as genome replication through a positive-strand intermediate (29, 66), which represents an essential step in the viral life cycle that is attractive for the development of antiviral therapeutics.

Of relevance to RSV's ability to induce LRT inflammation is the fact that RSV replication in epithelial cells induces the expression of cytokines (20, 23, 47), chemokines (5, 48, 67), arachidonic acid metabolites (24), and reactive oxygen species (10) and the cell surface display of major histocompatibility complex (MHC) class I (39). Recent studies applying macro- and high-density oligonucleotide arrays have indicated that RSV replication is a potent inducer of global genetic responses in infected lower-airway epithelial cells, influencing ~30% of the expressed cellular genes (e.g., the transcriptosome [59, 67]). Focused analysis of virus-induced chemokine production showed a time-dependent expression of the CC (I-309, Exodus-1, TARC, RANTES, MCP-1, MDC, MIP-1α, and MIP-1β), CXC (growth-regulated oncogenes [GRO] α, -β, and -γ; ENA-78; interleukin-8 [IL-8]; and I-TAC), and CX$_3$C (Fractalkine) subclasses (67). Moreover, mechanistic studies have shown that RSV replication is an inducer of the transcription factor nuclear factor κB (NF-κB), a master regulator of inflammation (4, 23, 59). RSV replication is required for NF-κB activation if the application of nonreplicating virus (5, 36) or of conditioned medium from RSV-infected cells (36) or the inhibition of RSV replication by the antiviral agent ribavirin fails to activate NF-κB (21) and downstream chemokine expression.

Ribavirin (1-β-D-ribofuranosyl-1,2,4-triazole-3-carboxamide) is a synthetic guanosine analog and is a nontoxic, broad-spectrum inhibitor of RNA and DNA viruses that is currently licensed for the treatment of severe RSV disease (15) as well as influenza (26) and chronic hepatitis C (17, 18). Although its primary mechanism of action is unclear, ribavirin accumulates intracellularly as mono- and triphosphate intermediates. Ribavirin monophosphate, a competitive inhibitor of IMP dehydrogenase, depletes cellular GTP, interfering with viral RNA capping reactions, whereas ribavirin triphosphate is incorporated by viral polymerase into RSV genomic transcripts, thus forcing "error catastrophe" and viral extinction (16, 26, 65). Because of its highly selective effect on viral replication, the effect of ribavirin on RSV-induced CXC chemokine (IL-8) and cytokine (IL-6) expression has been reported, and its short-term effect is to reduce the expression of both cytokines (21, 40). In the study of Fiedler et al., ribavirin's effect on NF-κB activation was also examined and it was shown to reduce both NF-κB's DNA binding and its transcriptional activity (21). In spite of its potent antiviral effect in vitro, ribavirin has met with only modest clinical success in the treatment of established RSV disease, having minimal or insignificant effects on mortality or the duration of hospitalization (reviewed in reference 65).

We applied high-density microarrays to investigate the effect of ribavirin treatment on the epithelial-cell genomic response. We hypothesized that the epithelial-cell genomic response to RSV would be modified by the inhibition of high-level RSV replication, and we sought to examine specifically whether RSV-induced chemokine responses were altered by antiviral treatment. The knowledge of these genetic responses to virus-drug interactions will help to further guide the improvement of antiviral-drug strategies.

MATERIALS AND METHODS

Cell culture and treatment. Human A549 pulmonary type II epithelial cells (American Type Culture Collection) were grown in Dulbecco minimal essential medium with 10% fetal bovine serum, penicillin (100 U/ml), and streptomycin (100 μg/ml) at 37°C in a 5% CO$_2$ incubator (59, 67). The human RSV A2 strain was grown in HEp-2 cells and purified by centrifugation on discontinuous sucrose gradients (61). The virus titers of the purified RSV pools ranged from 7.5 to 8.5 log PFU/ml, as determined by a methylcellulose plaque assay. No contaminating cytokines, including IL-1, TNF-α, IL-6, IL-8, granulocyte-macrophage colony-stimulating factor, and interferon (IFN), were found in these sucrose-purified viral preparations (23). Lipopolysaccharide, assayed by the Limulus hemocyanin agglutination assay, was also not detected. Virus pools were aliquoted, quick-frozen on dry ice-alcohol, and stored at −70°C until used. For viral adsorption, cells were then placed in Dulbecco minimal essential medium containing 2% (vol/vol) fetal bovine serum and infected with sucrose cushion-purified RSV (pRSV) at a multiplicity of infection (MOI) of 1 for 36 h prior to being harvested and assayed. Ribavirin was obtained from ICN Biochemicals (Aurora, Ohio) and dissolved in sterile distilled water at a concentration of 20 mg/ml. Unless otherwise stated, cells were pretreated with ribavirin at a final concentration of 100 μg/ml in culture medium for 2 h prior to viral adsorption.

Plasmid construction and transfection. The common promoter of the genes for transporter associated with antigen processing 1 (TAP-1) and and low-molecular-mass polypeptide (LMP2) (~600 bp) were amplified by PCR from A549 cell genomic DNA. The primers used were TAP-1–LMP2 sense, with the sequence 5′-AGGATCCCTGCAAGGCACCGCT-3′ (BamHI sequence underlined), and TAP-1–LMP2 antisense, with the sequence 5′-AAAGCTTGGCAC TCGGACGCC-3′ (HindIII restriction site underlined). The promoter was restricted and cloned into the BamHI and HindIII sites of the pOLUC reporter vector (9). The IFN-stimulated response element (ISRE) site of the TAP-1–LMP2 promoter was mutated by a two-step PCR technique involving gene splicing by overlap extension (8). In the first step, two fragments were produced by using the wild-type promoter as a template; fragment A contained the mutated ISRE site and the downstream region of the TAP-1–LMP2 promoter (produced by using a mutating sense primer containing the sequence 5′-GCGG CCGCTTTCGATCTACCTGTCCCCTAAATGGCTGAG-3′ and the TAP-1–LMP2 antisense primers), and fragment B contained the mutated ISRE site and the upstream region of the TAP-1–LMP2 promoter (produced by using a mutating antisense primer containing the sequence 5′-CTGCTCAGCCATTTAGG GGACAGGTAGATCGAAAGCGGC-3′ and the TAP-1–LMP2 sense primers) (underlining indicates the location of site mutations). In the second step, gel-purified fragments A and B were combined, and the TAP-1–LMP2 ISRE mutant promoter was reconstructed by using the fragments as templates in a PCR with the TAP-1–LMP2 sense and TAP-1–LMP2 antisense primers. The mutated promoter was restricted, cloned into the BamHI and HindIII sites of the pOLUC reporter, and sequenced to confirm its authenticity. The multimers of the LMP2–TAP-1 ISRE were made by annealing the oligonucleotides 5′-GATCGCTTTC GATTTCGCTTTCCC-3′ and 5′-GATCGGGAAAGCGAAATCGAAAGC-3′, phosphorylating them, and ligating them upstream of an inert TATA box driving firefly luciferase (−54/44 nucleotides of IL-8 promoter Luc[11]).

For transfection, approximately 10^6 A549 cells were plated in 6-cm-diameter tissue culture dishes in triplicate on the day before transfection. Each plate of cells was transfected with 2 μg of reporter plasmid and 1 μg of a cytomegalovirus–β-galactosidase (β-Gal) internal-control plasmid with FuGene 6 transfection reagents (Roche, Indianapolis, Ind.). Twenty-four hours later, cells were infected with RSV at an MOI of 1.0. At 15 h postinfection, cells were lysed and luciferase and β-Gal reporter activities were measured. Luciferase activity was normalized to internal-control β-Gal activity. The multiple of the increase in induction was calculated by dividing the normalized luciferase reporter activity in treated plates by that of the control.

Biotinylated pull-down and Western immunoblot assay. Microaffinity purification of ISRE binding proteins was performed as previously described (55) by using chemically synthesized ISRE wild-type oligonucleotides containing 5′ biotin (Bt) on a flexible linker (Genosys, The Woodlands, Tex.). Forty picomoles of duplex Bt-ISRE was incubated with 1 mg of sucrose cushion-purified nuclear extracts in the presence of 10 μg of poly(dI-dC) in a 1,000-μl volume of binding buffer (containing 8% [vol/vol] glycerol, 5 mM MgCl$_2$, 1 mM dithiothreitol, 100 mM KCl, 1 mM EDTA, and 12 mM HEPES [pH 7.9]) for 20 min at 25°C. Binding reaction mixtures were then centrifuged at 12,000 × g for 5 min at 25°C. Supernatants were aliquoted into fresh microcentrifuge tubes, and binding proteins were captured by the addition of 50 μl of a 50% (vol/vol) slurry of streptavidin-agarose beads (Pierce, Rockford, Ill.) for 5 min at 25°C with mixing. Beads were pelleted by centrifugation at 4,000 × g for 2 min at 25°C and washed two

TABLE 1. Primer pairs used for Northern blot hybridization

Gene	Product size (bp)	GenBank no.	Primer sequence (5'-3')	Strand
TAP-1	322	X66401	GGCTGGATCCCAGCTGTCAGGGGGTCAGC	Sense
			ATGAAGCTTCATTCTGGAGCATCTGCAGGAGCCTG	Antisense
LMP2	250	X66401	CTGGGATCCATGCTGACTCGACAGCCTTTGC	Sense
			GAAGAAGCTTCACTCATCATAGAATTTTGGCAGTTCATT	Antisense
IF1 6-16	320	U22970	GCAGCAGCGTCGTCATAGGT	Sense
			CGGCGCATGCTTGTAATCC	Antisense
p78	312	M33882	ACCAGCGACAAGCGGAAGT	Sense
			AGCATCCTTCAATCCCGCC	Antisense
IFI 9-27	321	J04164	CATGTCGTCTGGTCCCTGTTC	Sense
			GCCAGCATTGCACAGTGGA	Antisense
STAT-1	441	M97935	GAGGAGTCCACCAATGGCA	Sense
			CACGGAATGAGACCATCGG	Antisense
IRF-7B	304	U53831	GGCAAGTGCAAGGTGTACTGG	Sense
			GGAAGACACACCCTCACGCT	Antisense

times in binding buffer. ISRE binding proteins were then eluted with a 1× sodium dodecyl sulfate (SDS)-polyacrylamide gel electrophoresis loading buffer for Western immunoblot analysis.

For Western immunoblotting, eluted proteins were fractionated by SDS–10% polyacrylamide gel electrophoresis and transferred to polyvinylidene difluoride membranes (Millipore, Bedford, Mass.) (38). Membranes were blocked in a solution containing 5% milk–Tris-buffered saline and 0.1% Tween 20 for 1 h and immunoblotted with affinity-purified anti-STAT-1 rabbit polyclonal antibody (Santa Cruz Biotechnology, Santa Cruz, Calif.) for 1 h at 4°C. Membranes were washed four times in Tris-buffered saline–0.1% Tween 20 and incubated with horseradish-peroxidase-conjugated anti-rabbit immunoglobulin G for 1 h. Immune complexes were detected by reaction in an enhanced-chemiluminescence assay (ECL;Amersham) according to the manufacturer's recommendations.

cDNA probes. A549 mRNA was reverse transcribed with Superscript II and with oligo(dT) used as a primer according to the recommendations of the manufacturer (Gibco/BRL). Partial cDNAs of TAP-1, LMP2, IFI 6-16, MxA/p78, IFI 9-27, STAT-1, and IRF-7B were amplified in the PCR using A549 cDNA as a template and the primers indicated in Table 1. All cDNAs were sequenced to confirm authenticity. Probes were radiolabeled by using asymmetric PCR amplification of the cDNA with the corresponding antisense primer and purified by gel filtration chromatography (39).

Northern blot analysis. Total cellular RNA was extracted by acid guanidium-phenol extraction (Tri Reagent; Sigma). RNA (20 μg) was denatured, fractionated by electrophoresis on a 1.2% agarose-formaldehyde gel, capillary transferred to a nitrocellulose membrane (Zeta-ProbeGT; Bio-Rad), and prehybridized as described previously (8). The 1.1-kb RSV N cDNA probe was produced by PCR with poly(A)+-primed cDNA from RSV-infected A549 cells as a template and with the sense primer 5'-CAAATGGATCCATGGCTCTTAGCAAAGTCAA G-3' and the antisense primer 5'-TTCCCGGTTCAAAGCTCTACATCATTA TC-3'. The RSV N cDNA probe was produced by using asymmetric PCR of the RSV N plasmid with the antisense primer and purified by gel filtration chromatography. The membrane was hybridized with 1 × 10⁶ to 2 × 10⁶ cpm of ³²P-RSV-N cDNA probe per ml at 60°C overnight in 5% SDS hybridization buffer. The membrane was washed with a buffer containing 5% SDS and 1× saline-sodium citrate (0.15 M NaCl and 0.015 M sodium citrate) for 20 min at room temperature followed by 30 min at 60°C. Internal-control hybridization was performed with 18S RNA. The membrane was exposed to XAR film (Kodak) for 70°C and quantified by exposure to a PhosphorImager cassette.

Oligonucleotide probe-based microarrays. The Hu95A GeneChip (Affymetrix, Inc., Santa Clara, Calif.) containing 12,625 sequenced human genes was used as previously described (67). Briefly, first-strand cDNA synthesis was performed by using total RNA (10 to 25 μg), a T7-(dT)₂₄ oligomer [5'-GGCCAGTGAATTG TAATACGACTCACTATAGGGAGGCGG-oligo(dT)₂₄-3'], and SuperScript II reverse transcriptase (Life Technologies). The T7 promoter introduced during first-strand cDNA synthesis was then used to direct the synthesis of cRNA by using bacteriophage T7 RNA polymerase. The Bt-labeled target RNAs were fragmented to a mean size of 200 bases and initially hybridized to a test array containing a set of probes representing genes that are commonly expressed in the majority of cells (actin, GAPDH [glyceraldehyde-3-phosphate dehydrogenase], transferrin receptor, transcription factor ISGF-3, 18S RNA, 28S RNA, and alu) to confirm their successful labeling. Hybridization was performed at 45°C for 16 h in a hybridization buffer (0.1 M MES [morpholineethanesulfonic acid, pH

6.6], 1 M NaCl, 0.02 M EDTA, and 0.01% Tween 20). Four prokaryotic genes (bioB, bioC, and bioD from the E. coli Bt synthesis pathway and cre, the recombinase gene from P1 bacteriophage) were added to the hybridization cocktail as internal controls. Gene chips were washed under both nonstringent (1 M NaCl, 25°C) and stringent (1 M NaCl, 50°C) conditions prior to being stained with phycoerythrin streptavidin (final concentration, 10 μg/ml). Gene chip arrays were scanned with a gene array scanner (Hewlett-Packard) and analyzed with the GeneChip Analysis Suite 4 software (Affymetrix, Inc.).

Statistics and data analysis. For comparison of the fluorescence-intensity (average difference) values among multiple experiments, the average-difference values for each experimental gene chip were normalized to that of the base gene chip. This was done first by calculating the 2% trimmed mean (a measurement of global signal intensity) for each probe set considered to be present on the gene chip. The trimmed mean is obtained by calculating the mean signal intensity of the chip after discarding the highest and lowest 2% average-difference values (representing the outliers). Normalization was performed by multiplying all the average differences of genes considered present in the experimental array by a global normalization factor defined as the ratio of the base trimmed mean to that of the experimental trimmed mean (the base chip was considered to be the first control gene chip). In the case of a probe set considered absent, the machine background value was substituted. To evaluate reproducibility, pairwise comparison of the fluorescence-intensity value for each probe set was performed by least-squares linear-regression analysis for each treatment group. To identify genes influenced by either ribavirin or RSV, the ribavirin treatment and RSV infection were considered independent experimental manipulations. Here, the scaled average-difference values were then subjected to a two-way analysis of variance with replications (ANOVA; Splus 6; Insightful, Inc.). P values [probability of the F ratio $Pr(F)$] at the <0.01 confidence level as a result of either treatment were deemed highly significant, and genes (probe sets) with these values were selected for further analysis. Agglomerative hierarchical clustering by the unweighted-pair group method with arithmetic means (59) was performed on the indicated genes (Spotfire Array Explorer, version 7; Spotfire, Inc., Cambridge, Mass.). Data are graphically presented as heat maps, where fluorescence intensity is represented by a color gradient. For the heat maps shown, green represents the minimum average-difference value (100 scaled units), black represents the middle average-difference value (5,000 scaled units), and red represents the maximum average-difference value (10,000 scaled units). Investigators may obtain the primary data from our website (http://bioinfo.utmb.edu/Brasier _Lab). For calculations of the multiple of the increase, the mean normalized average-difference intensity for each treatment was divided by the mean control average-difference intensity. In situations where the control probe set was considered absent, the machine background value was substituted.

RESULTS

Dose-response studies. In RSV-infected epithelial cells, ribavirin reduces plaque formation, the release of infectious virions, and F glycoprotein expression in a dose-dependent manner over the range of 10 to 100 μg/ml without cellular toxicity in culture for up to 7 days (21, 35). To determine the
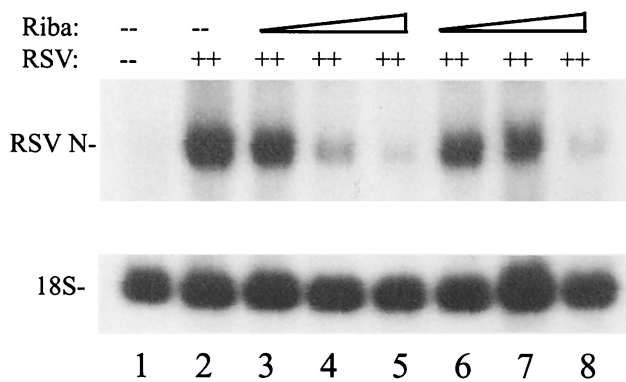
FIG. 1. Treatment of epithelial cells with ribavirin. Northern blot of the RSV N transcript from uninfected (lane 1) or pRSV-infected (MOI, 1) (lanes 2 to 8) A549 cells. Cells were pretreated with ribavirin (Riba; 100 μg/ml for 2 h) prior to viral adsorption (lanes 3 to 5) or posttreated with ribavirin (1 h) after viral adsorption. Concentrations of ribavirin used were 0 μg/ml (lanes 1 and 2), 10 μg/ml (lanes 3 and 6), 32 μg/ml (lanes 4 and 7), and 100 μg/ml (lanes 5 and 8). Bottom panel, rehybridization with the 18S probe.

optimal concentration and timing of ribavirin treatment for the inhibition of viral transcription for our studies, A549 monolayers pretreated (2 h) or posttreated (1 h) with increasing concentrations of ribavirin were exposed to pRSV. Total cellular RNA was harvested 36 h later, and the abundance of the 1.1-kb RSV N transcript was measured by Northern blotting (Fig. 1). Compared to mock-infected cells, cells exposed to pRSV for 36 h in the absence of ribavirin had a strong induction of the RSV N transcript (Fig. 1, top panel, compare lanes 1 and 2). In contrast to the negligible effect of ribavirin at 10 μg/ml, the 32-μg/ml dose significantly, but not completely, inhibited RSV N transcription (compare lanes 2, 4, and 7). At the 32- and 100-μg/ml doses of ribavirin, the cells that had been pretreated with ribavirin had significantly fewer N transcripts than the cells treated with ribavirin 1 h after viral exposure (compare lanes 4 and 7 and lanes 5 and 8, Fig. 1). As a control for total RNA recovery, the same RNA samples were hybridized to 18S RNA, where an equal hybridization signal was observed (Fig. 1, lower panel). At an MOI of less than 1.0, 100 μg of ribavirin per ml reduced RSV N transcript abundance to 13% ± 7% of that observed in non-ribavirin-treated cells (data not shown) These data indicated that significant inhibition of RSV transcription could be attained by pretreatment with ribavirin at a 100-μg/ml concentration and was selected as the condition for subsequent experimentation.

High-density microarray analysis. To identify how ribavirin modified the genetic response to RSV infection, we harvested RNA from control or ribavirin-treated cells in the absence or presence of pRSV infection and profiled mRNA abundance using high-density oligonucleotide arrays containing 12,625 sequenced human genes (Hu95A GeneChips; Affymetrix). For each treatment group, pairwise comparison of the fluorescence-intensity values was carried out by least-squares linear-regression analysis; for the control chips, the regression yielded a slope (m) of 1.04 ($r^2 = 0.99$), indicating that the hybridization intensity measurements for each gene were highly reproducible (Fig. 2A). Similar data were observed for the pairwise comparison of values from ribavirin treatment ($m = 1.04$, $r^2 =$

0.99), RSV infection ($m = 0.86$, $r^2 = 0.96$), and ribavirin plus RSV treatments ($m = 0.97$, $r^2 = 0.99$; data not shown). To compare the global cellular genetic responses after the various treatments, the gene chip data were subjected to hierarchical-clustering analysis. In this technique, the gene expression profile after each treatment is grouped with its nearest neighbor and the mathematical proximity of these gene expression profiles is indicated by the height of a common line that connects the two nodes. As seen in Fig. 2B, the gene expression profile for each condition clustered with that of its own replicate. Importantly, the results of the control and ribavirin treatments were quite similar, as is indicated by the short vertical line connecting the two data sets. Conversely, the genetic profile from RSV infection and that from combined ribavirin treatment with RSV infection were distinct from the control and ribavirin profiles and from each other. Together, these data indicated that we had obtained a robust and reproducible data set and that the genetic responses to ribavirin treatment alone were minimal but that RSV infection (with or without ribavirin treatment) had the greatest impact on the global gene expression profile.

Effect of ribavirin on the epithelial-cell genetic response to RSV infection. Two-way ANOVA was then used to identify genes whose expression levels were statistically significantly altered by RSV infection or by ribavirin treatment [for this analysis, we accepted genes whose Pr(F) values were <0.01 to minimize the number of false-positive results in our analysis]. In earlier reports, we classified the RSV-regulated genes by putative function (67). Here, we found that RSV infection perturbs the expression of genes controlling multiple biological pathways, including cytokines and chemokines, growth factors, putative antiviral factors, receptors, cellular structure, DNA repair and chromosomal maintenance, histocompatability and cell surface markers, metabolism, oncogenes, RNA processing and protein translation, secreted peptides, signaling molecules and kinases, transcription factors, and those of unknown function. In this study representing a static measurement taken 36 h after pRSV exposure, we found that the expression levels for a total of 3,233 genes (representing 49% of the expressed genes) were significantly altered by RSV infection and that 272 genes (representing 4% of the genes considered present on the chip) were influenced by ribavirin treatment. Figure 3A shows a Venn diagram of the relationship of these two data sets. We noted that the majority (89%) of the genes that were affected by ribavirin treatment were also regulated by RSV. These data suggest that ribavirin has a minimal impact on constitutive gene expression on the airway epithelial cell, a finding consistent with its low cellular toxicity, and that the global gene expression profiles of ribavirin and control cells cocluster (Fig. 2B). Conversely, only 7.5% of the total genes inducible by RSV were modulated by ribavirin treatment. These data suggest that the epithelial-cell genetic response to RSV is largely independent of high levels of viral transcription. The expression patterns and functional activities of the genes influenced by both treatments were further analyzed.

To visually compare the changes in mRNA abundance for the 241 genes found to be influenced by RSV infection and ribavirin treatment, hierarchical-clustering analysis was performed. The normalized primary data are represented as a heat map with a color coding scheme to represent the hybrid-
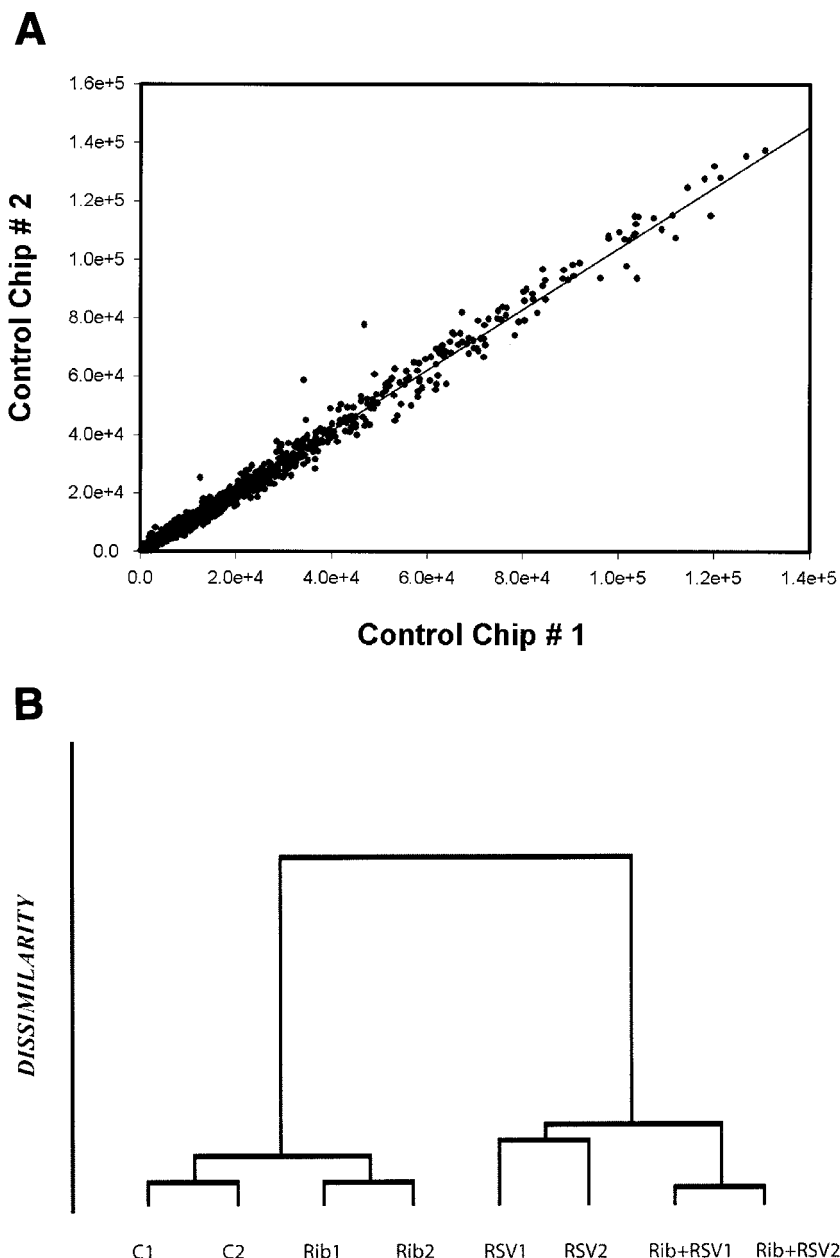
A

B

FIG. 2. Analysis of GeneChip data set. (A) Reproducibility of hybridization intensity. As a measure of experimental reproducibility, the fluorescence intensity (normalized average difference value) for each probe set present on the gene chip was plotted in one experiment to its value in the second. Least-squares linear-regression analysis was used to determine the relationship between the two data sets. The data could be described by a straight line with a slope of 1.04 ($r^2 = 0.99$). Further, of the 12,625 probe sets present on the chip, $6,651 \pm 290$ had hybridization signals that were significantly above background and were considered present. This value did not deviate by more than 4% across the different treatment groups, indicating that neither the drug treatment nor viral infection had global effects on the performance of the gene chip. (B) Agglomerative hierarchical-clustering analysis for each treatment condition was performed by using the unweighted-pair group method with arithmetic means technique (as described in Materials and Methods). Note that the results for each treatment condition most closely cluster with those for its independent replicate. C1 and C2, first and second controls, respectively; Rib1 and Rib2, first and second treatments with ribavirin, respectively; RSV1 and RSV2, first and second treatments with RSV, respectively.

ization intensity for each gene. As seen in Fig. 3B, four major genetic responses were observed: group I was strongly up-regulated by RSV and its RSV-induced expression was significantly inhibited by ribavirin treatment, group II was a group of genes strongly up-regulated by RSV infection and whose expression was further increased by ribavirin treatment, group III was slightly down-regulated by ribavirin and further down-regulated by RSV infection, and group IV was slightly induced by ribavirin treatment and down-regulated by RSV infection. Because of the interesting behavior and functional activity of the first two groups, they will be further analyzed here (the complete data set is available on our website).
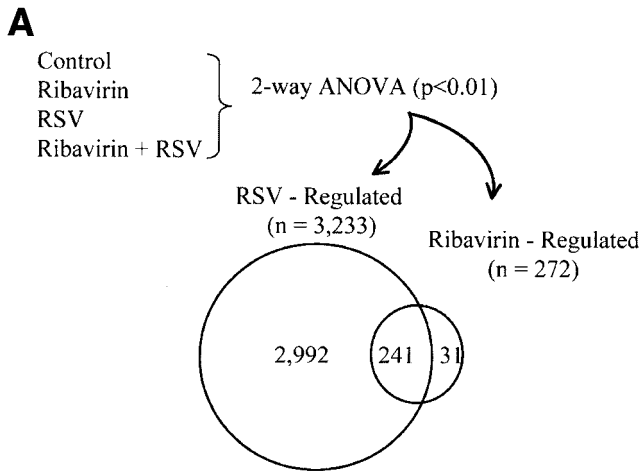
A

FIG. 3. Relationships between sets of genes regulated by RSV infection or ribavirin treatment. (A) Venn diagram showing the intersections between RSV and ribavirin-regulated genes in A549 cells. Two hundred forty-one genes were common to both data sets. (B) Hierarchical clustering and heat map of the 241 genes common to both treatment groups. The left section is the dendrogram produced by gene expression profiles. The middle section is the heat map, based on hybridization intensity (green is 100, black is 5,000, and red is 10,000 fluorescence intensity units). The right portion is vertical lines that indicate the four distinct gene expression patterns, labeled I to IV. Group I genes are those that are RSV inducible but inhibited by ribavirin (Table 2). Group II genes are those that are RSV inducible and further enhanced by ribavirin (Table 3). C1 and C2, first and second controls, respectively; Rib1 and Rib2, first and second treatments with ribavirin, respectively; RSV1 and RSV2, first and second treatments with RSV, respectively; R+R1 and R+R2, first and second treatments with ribavirin and RSV, respectively; R+R1 and R+R2, first and second treatments with ribavirin and RSV, respectively.

B
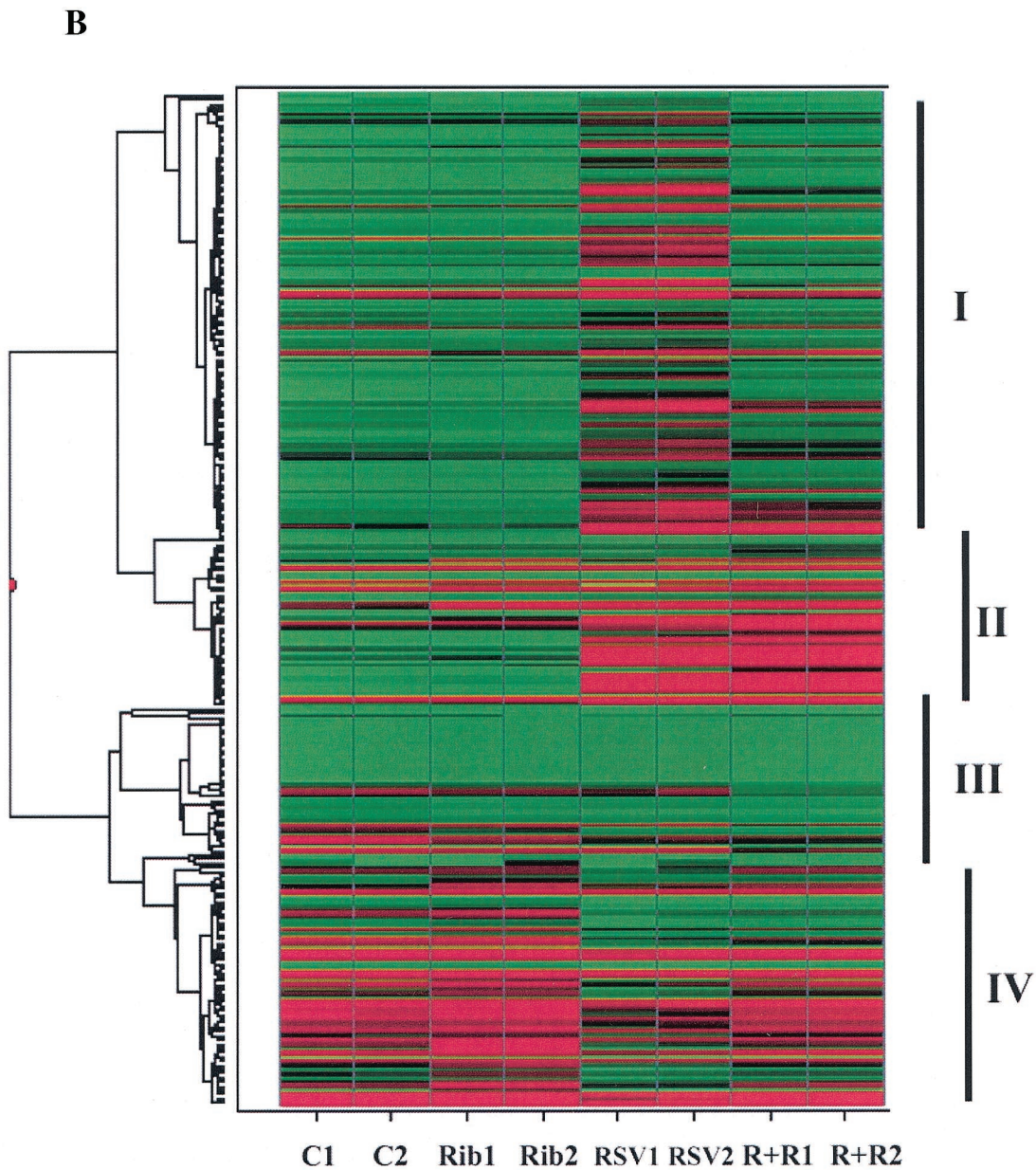
We retrieved the predicted amino acid sequences for the genes present in the group I gene cluster and classified them by putative biological function. For genes encoding proteins of unknown function, BLAST searches were performed with sequences in the human genome database to aid in their classification. Of the 114 genes present, the function of 58 could be assigned (Table 2; the unknown genes are indicated in the footnote of the table). These genes represent a wide range of biological activities, including those involved in cell cycle control, immunoregulation (cytokines and chemokines), growth, metabolism, intracellular signaling (kinases), and genetic response (transcription factors). We noted that the CC chemokines MIP-1α and -1β were inhibited by ribavirin in the context of RSV infection. The effect of ribavirin on the expression of cell surface receptors, including the adenosine A2 receptor and the prostaglandin E2 (pEG2) receptor as well as the signaling molecules, suggests that ribavirin influences the responsiveness of RSV-infected cells to other stimuli. Finally, we noted the reduction in expression of a number of transcription factors, including two independent probe sets for c-jun and a basic domain leucine zipper containing a member of the activating protein 1 (AP-1) complex. AP-1 is an RSV-inducible transcription factor that partially mediates promoter induction by RSV (12).

We were surprised that the expression of more chemokines was not influenced by ribavirin treatment, especially since others have shown that ribavirin treatment inhibits IL-8 expression (21). To specifically examine the effects of ribavirin on chemokine expression by RSV-infected epithelial cells, we retrieved the expression profiles for all 14 chemokines known to be RSV inducible that were present on the chip (67). These data are clustered and presented visually as heat maps in Fig. 4, where the expression patterns in response to RSV infection or treatment with ribavirin can be seen. For example, the levels of abundance of MIP-1α and -1β transcripts are low or undetectable in control or ribavirin-treated cells (indicated by the green color) and are strongly induced by RSV replication in RSV-infected cells, in which the intensity of hybridization is high (indicated by red). In the presence of ribavirin, RSV-induced expression was inhibited. We noted that GRO-γ seemed to have a similar qualitative profile, but because of the variation between replicates, GRO-γ was not identified by the ANOVA to be statistically significantly regulated by ribavirin treatment. Importantly, the remaining chemokines, including members of both the CC (Exodus-1, RANTES) and CXC (GRO-α, -β, and -γ; ENA-78; and IL-8) subclasses were strongly induced by RSV infection and apparently were not affected by ribavirin treatment. At present, we cannot reconcile our findings with those of other reports that ribavirin inhibits IL-8 expression; these differences may be due to the dosing or timing of viral infection. Together, our data indicate that epithelial-cell chemokine synthesis is largely preserved by ribavirin treatment. That the epithelial cell still robustly synthesizes inflammatory chemokines even when viral replication is reduced by ~90% may, in part, account for some of the apparent lack of clinical effect.

Ribavirin up-regulates expression of antiviral genes in RSV-infected cells. We were particularly interested in the analysis of group II genes, genes whose expression was up-regulated by combined ribavirin treatment and RSV infection, which were classified according to putative biological function (Table 3). Of the 45 genes in this group, we tentatively identified the functions of 31. The spectra of biological pathways for these genes were quite distinct from those of the ribavirin-inhibited gene set. Here, cytoskeletal, metabolic, and secreted proteins and transcription factors were the major biological pathways identified. We were surprised that the list was predominated by putative antiviral genes and ISGs. This was a surprising finding because IFN-β, the only IFN expressed by A549 cells in response to RSV (39, 67), was identified to be ribavirin down-regulated (Table 2). For example, the IFN-inducible peptide 6-16 is strongly inducible by type I IFNs through a *cis*-regulatory ISRE in its promoter (49); the antiviral genes MxA/p78 and the IFN-inducible 56-kDa protein were cloned as type I IFN-inducible genes (34, 63). Similarly, fibrinogen and the complement proteins H and C1r (part of the secreted-protein group) are strongly inducible by IFN-γ in other cell types (62). These common modes of regulation were particularly significant because IFN-activated transcription factors, such as STAT-1 and IRF-7, were also in group II, classified as the transcription factor pathway (Table 3).

To independently validate the surprising findings that expression of IFN-inducible genes are further induced in the presence of ribavirin, we performed Northern blot hybridizations of similarly treated control, ribavirin-treated, RSV-infected, and RSV- and ribavirin-treated cells using probes specific for IFI 6-16, IFI 9-27, MxA/p78, STAT-1, and IRF-7B transcripts. As shown in Fig. 5A, transcripts encoding IFI 6-16, IFI 9-7, and MxA/p78 were undetectable in control cells. Ribavirin treatment did not detectably influence the expression levels for any of these mRNA species. RSV infection strongly up-regulated the expression for all of these transcripts. Finally, the treatment of RSV-infected cells with ribavirin increased IFI 6-16, IFI 9-27, MxA/p78, STAT-1, and IRF-7B expression 2.6-, 4.7-, 2.9-, 1.4-, and 1.7-fold, respectively, over that induced by RSV alone. These data confirm the results of the microarray studies. Although not appearing in the ribavirin-up-regulated group at this level of statistical significance, we have previously shown that RSV is a potent up-regulator of TAP-LMP2 and their gene loci in the MHC class I complex through a mechanism involving the secretion of IFN-β (39). Using TAP-LMP2 as a well-characterized, independent target for IFN signaling, we investigated whether ribavirin also up-regulated its expression. Northern blot analysis was performed on RNA from control or RSV-infected cells in the absence or presence of ribavirin (Fig. 5B). As previously described, RSV strongly induced 2.8-kb TAP-1 and 0.9-kb LMP2 transcript abundance (39). Although ribavirin treatment alone did not induce TAP-1 or LMP2 expression, ribavirin further induced their expression (Fig. 5B) in the presence of RSV replication. These observations suggested that the IFN-signaling pathway was enhanced by ribavirin treatment combined with RSV replication.

Ribavirin potentiates ISRE-dependent transcription and STAT-1 binding. Previous work has shown that TAP-LMP2 expression is controlled by a bidirectional promoter containing an IFN-inducible ISRE element that binds STAT-1 (13, 14, 46). We next determined whether TAP-1–LMP2 transcription was enhanced by ribavirin treatment. A549 cells were transiently transfected with the TAP-1–LMP2 luciferase reporter and treated with ribavirin in the absence or presence of RSV.

TABLE 2. Functional classification of ribavirin-down-regulated genes[a]

Function and protein	GB No.	Location on clustering diagram	MC1	MC2
Apoptosis or cell cycle proteins				
Caspase-like protein	AF005775	94	3.80	3.03
Cdc14	AF000367	38	6.55	0.71
Cytokines				
IL-15	U14407	27	6.05	1.81
IL-15	AF031167	28	4.16	1.41
MIP-1α	D90144	18	192.29	47.76
MIP-1β	J04130	66	43.02	17.02
IFN-β1	V00535	91	32.94	19.06
Cytoskeletal protein				
Alpha-tubulin	X06956	22	1.96	1.25
Annexin V	U05770	30	2.24	1.17
Caveolin-2	AF035752	44	1.55	0.93
Beta-tubulin	X79535	36, 8, 19	3.67	1.33
DNA repair or chromosomal protein				
CENPC	M95724	58	1.91	1.27
Growth factors or secreted proteins				
bFGF	M27968	69	5.41	2.82
PTH-like protein	M24351	77	3.69	2.73
VEGF related	U43142	78	6.43	3.95
PA1-I	M14083	98	3.98	3.64
Metabolism proteins				
Cathepsin E	M84424	14	10.12	2.74
Deacetylase	L32179	57	1.98	1.30
UbcH5C	U39318	81	1.57	1.32
ADP ribosylation factor	U73960	33	2.85	1.20
CYP1B1	U03688	12	9.24	3.41
Ca^{2+}-pumping ATPase	J04027	112	1.01	0.72
p67-phox	M32011	64	21.77	9.22
Receptor proteins				
4-1B	U03397	16	40.29	9.27
PGE2 receptor	U19487	61	9.35	5.29
GPCR	X95876	2	1.35	0.94
AH receptor	L19872	62	4.46	2.17
Adenosine A2 receptor	S46950	68	69.62	28.79
Axl	M76125	74	3.05	2.23
IL-2 receptor gamma	D11086	87	26.34	15.50
Signaling proteins				
STE20 homolog	U77129	21	2.23	1.34
PP1	Y18207	37	6.12	0.75
Rap1GEF	AF103905	39	7.55	0.71
Kinase	AF059617	43	2.03	0.90
Calcineurin A cat sub.	S46622	29	3.44	1.30
Ral	U14417	56	2.06	1.39
Ras-like protein	M31468	54	1.58	1.34
STAT inhibitor 2	AF037989	20	7.37	2.69
Phosphatase MKP-5	AB026436	67	53.12	7.07
Smad1	U59423	72	2.29	1.62
Smad1	U59912	75	2.58	1.91
RanGTPase activator	X82260	79	2.09	1.62
TNF receptor 2 associated	U12597	76	27.46	17.90
GTPase activating	AF060877	7	6.05	2.02
Gem GTPase	U10550	40	4.29	1.13
IP3 receptor	U01062	82	2.14	1.47
Transcription factors				
E2F related	L23959	115	0.82	2.55
Forkhead	AF032886	11	2.74	1.42
c-jun	J04111	17	83.53	7.66
c-jun	J04111	13	16.41	4.26
YY1 associated	U72209	50	1.44	1.06
IRF-5	U51127	102	1.46	0.81
Human GATA3	X58072	60	7.01	3.36
Zn homeodomain	L32832	80	1.61	1.30

[a] Functional classification of ribavirin-down-regulated (group I) genes. The records for each gene identified in Fig. 3B were tabulated and classified by functional activity (biological pathway). For each, the common name, the reference location in the cluster, the GenBank accession number (GB no.), the location on the clustering diagram, and the multiple of the change (MC) in signal intensity relative to that of untreated cells are indicated. MC1 is the mean average difference for RSV-infected cells divided by that for untreated cells. MC2 is the mean average difference for ribavirin-treated and RSV-infected cells divided by that for untreated cells. Identical entries indicate independent probe set representation on the GeneChip. GenBank accession numbers of genes present in this group with unknown functions (with locations on the clustering diagram in parentheses) are AA478904 (3), AJ001685 (4), U19261 (5), AJ001684 (6), AI800499 (9), X63741 (10), AI765533 (15), Y11307 (23), U50527 (24), AB023157 (25), AB020700 (26), N36638 (32), X63417 (34), D14533 (35), M80899 (41), M31166 (42), D50917 (31), N32859 (45), AF062075 (46), AB015331 (47), D82351 (48), AL050144 (49), AA114830 (51), AB007870 (52), AL096715 (53), AB002315 (55), AB007930 (59), AB023155 (63), AL049787 (65), AB023137 (70), AL021977 (71), AI674208 (73), AF070569 (83), X85785 (84), U46023 (85), W28205 (86), AF027866 (88), U27467 (89), AF099935 (90), AF055581 (92), AC004131 (93), AB013382 (95), U61849 (96), D83785 (97), D90070 (99), Z18948 (101), AL021707 (103), AA586695 (104), AL049940 (105), AB018293 (106), AB014563 (107), U38964 (108), S81439 (109), AF050110 (110), AB020645 (111), AB029039 (113), and D64015 (114). CENPC, centromere protein C; bFGF, basic fibroblast growth factor; PTH, parathyroid hormone; VEGF, vascular epithelial growth factor; GPCR, G-coupled receptor; AH, aryl hydrocarbon; GEF, guanine nucleotide exchange factor; Cat. sub., catalytic subunit; ranGTPase activator, Ras-related regulatory protein GTPase activator; Gem, GTPase from mitogen-induced T cells.
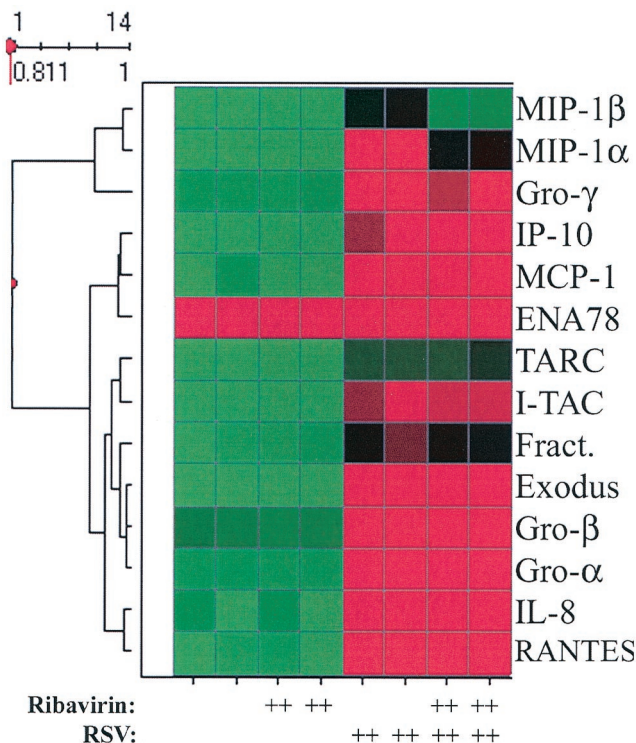
FIG. 4. Hierarchical clustering and heat map of the RSV-inducible chemokines. The gene expression data for 16 chemokines previously shown to be inducible by RSV were retrieved from the original data set (67). The data are as described in the legend to Fig. 3, with a cluster dendrogram at left and a heat map based on hybridization intensity (green is 100, black is 5,000, and red is 10,000 fluorescence intensity units) in the middle. Common names are indicated at right. Fract., fractalkine.

As seen in Fig. 6A, RSV replication induced a statistically significant 1.7-fold increase in normalized luciferase activity relative to that of untreated and uninfected controls. Although ribavirin did not induce reporter activity by itself, in the setting of viral replication, a further statistically significant increase in reporter activity was seen (Fig. 6A). The TAP-1–LMP2 promoter containing a site mutation in the ISRE was not inducible by RSV and not potentiated by the combined treatment with ribavirin. Together, these data suggested that ribavirin-enhanced up-regulation of TAP-1–LMP2 expression was, in part, transcriptional and that this effect required the action of the ISRE. To further determine whether the ISRE site was the target for ribavirin enhancement of TAP-1–LMP2 transcription, we tested a reporter gene driven by multimeric copies of the TAP-1–LMP2 ISRE. RSV replication was a potent inducer of ISRE-dependent transcription, increasing normalized luciferase activity 98-fold relative to that of uninfected cells (Fig. 6B). ISRE-dependent transcription in the ribavirin-treated, RSV-infected cells was induced 170-fold relative to that of the control. These data strongly indicated that ribavirin potentiated ISRE-dependent transcription.

Finally, we examined whether enhanced ISRE-dependent transcription was mediated through increased binding of STAT-1, a transcription factor that was identified to be up-regulated by ribavirin in the presence of RSV (group II genes

in Table 3). A specific biotinylated DNA pull-down assay was used to quantify the amount of STAT-1 binding to the TAP-1–LMP2 ISRE. In brief, nuclear extracts from control or treated cells were isolated and used to bind a biotinylated ISRE sequence (46). After ISRE binding proteins were captured on streptavidin beads, the beads were washed and associated proteins were fractionated and detected by Western immunoblotting with antibodies to STAT-1. This assay has been shown to be sequence specific and quantitative (8, 38, 55). As seen in Fig. 7, RSV induced the binding of STAT-1α and -1β isoforms to the TAP-1–LMP2 ISRE, a feature consistent with STAT-1α and -1β's enhanced mRNA expression detectable by microarray analysis. Further induction of DNA binding by the STAT isoforms was seen in the cells treated with ribavirin. Together, these data indicate that ribavirin induces ISRE-dependent transcription through a mechanism that, at least in part, involves enhanced STAT-1 recruitment to the ISRE.

DISCUSSION

The airway epithelium forms a cellular barrier between the external environment and internal milieu and plays an initiating role in pulmonary inflammation after exposure to environmental or infectious agents (reviewed in reference 45). In naturally acquired infections in humans, and in experimental infections of rodents, RSV is a potent inducer of airway inflammation and postinfectious airway hyperreactivity (2, 30; reviewed in reference 31). High-density mRNA profiling studies have yielded significant insights into the epithelial genomic response to respiratory viral infection (59, 67). RSV is a potent modifier of epithelial-cell transcriptosome, significantly influencing ~49% of the detected genes. RSV replication influences multiple biological pathways, including inflammatory responses through cytokine and chemokine expression, local antiviral responses, changes in cellular structure, alterations in DNA repair and chromosomal maintenance, induction of histocompatability complex and cell surface markers, switches in metabolism, expression of oncogenes, changes in RNA processing and protein translation, and changes in intracellular signaling (kinases and transcription factors). The ability of RSV to induce the expression of 17 distinct chemokines in type II alveolus-like epithelial cells (67) strongly argues for a central role for the epithelial cell in coordinating the inflammatory response to this virus. Here, we have applied high-density microarray analyses to empirically describe virus-drug interactions and understand the effect of ribavirin in modulating the epithelial-cell genomic response to RSV replication.

Ribavirin is a well-characterized potent antiviral agent able to inhibit RSV transcription, glycoprotein expression, syncytium formation, and virion release (references 21 and 35 and this study), yet it is largely devoid of cellular toxicity. Others have shown that continuous exposure of airway cells to ribavirin for up to 1 week produces no detectable toxicity as measured by cell growth or release of lactate dehydrogenase into the culture medium (21, 35). Our microarray data are consistent with these findings in that ribavirin treatment alone has only minor effects on epithelial gene expression, influencing the expression of only 31 genes (by twofold or less, ca. 0.5% of the total genes). Moreover, ribavirin did not affect overall

TABLE 3. Characteristics of ribovirin-up-regulated genes, gene products, and biological pathways[a]

Function and descriptor of protein or gene	GB no.	Location or clustering diagram	MC1	MC2
IFI or putative antiviral proteins				
IFI 6-16	U22970	145	112.98	206.89
MxA/p78	M33882	148	199.67	353.66
IFI 56 kDa	M24594	150	385.07	663.74
1-8U gene from IFI	X57352	151	11.27	18.78
IFI 9-27	J04164	156	267.59	535.82
p27	X67325	157	459.67	894.79
Cytoskeletal proteins				
Connexin 43	M65188	124	0.85	4.65
TAPA-1	M33680	127	1.05	1.53
MIC2	M16279	129	0.99	1.41
HSP70-2 gene (HLA)	M59830	135	6.44	10.30
Myosin heavy chain SM2	AF013570	143	36.62	56.62
Oncogene *pim-2h*	U77735	122	1.31	1.86
Metabolism proteins				
Trypsinogen C	U66061	126	0.85	24.47
Glutathione peroxidase-like	X53463	133	1.14	3.38
Argininosuccinate synthetase	X01630	136	2.56	3.70
NES1	AF055481	139	25.50	73.10
ALDHI	X05409	141	1.32	1.74
Secreted proteins				
Complement factor H	X07523	117	5.25	48.24
Neurite outgrowth-promoting protein	X55110	119	2.85	15.38
S-protein	X03168	121	1.72	6.47
Fibrinogen alpha	M64982	128	0.74	3.21
Apolipoprotein L	AF019225	144	51.20	77.01
C1r	M14058	149	4.72	7.60
C1r complement	J04080	159	3.44	4.66
Signaling protein LIM domain protein (CLIM1)	U90878	137	2.12	2.62
Transcription factors				
T-cluster binding protein	D64015	114	1.09	0.75
E2F related (DP-1)	L23959	115	0.85	2.62
SOX9	Z46629	120	1.18	1.92
STAT-1	M97936	147	5.78	9.80
IRF-7B	U53831	154	16.66	34.44

[a] For each gene, the common name, the reference location in the cluster, the GenBank accession number (GB no.), and the chromosomal locus are indicated. MC1 and MC2 are as described for Table 2. ALDHI, mitochondrial aldehyde dehydrogenase; LIM, *lin-11/isl-1/mec-3*. GenBank accession numbers (with location on the clustering diagram in parentheses for genes present in this group with unknown functions are: M94250 (146), U09196 (142), AA203487 (153), Y07828 (152), L78833 (155), D21853 (123), U58516 (118), X75918 (158), W25875 (125), H68340 (160), AL050282 (130), AA131149 (131), AI362017 (132), AC004877 (116), AB020687 (134), AL050267 (138), and AI762213 (140).

cellular gene expression profiles, as seen by the agglomerative clustering analysis (e.g., the ribavirin-treated cells coclustered with control cells in Fig. 2B). Together, these two observations indicate that the pharmacologic actions of ribavirin, including intracellular GTP depletion by IMP dehydrogenase inhibition, does not disturb genetic networks in uninfected epithelial cells.

Instead, we have found that the major impact of ribavirin is on the RSV-induced genomic response. Mechanistic studies have shown that RSV replication induces genetic networks through multiple pathways, including those upstream of the NF-κB, AP-1, CREB/ATF, STAT/IRF, and NF–IL-6 transcription factors (12, 21, 36, 37, 58, 59). We were surprised to find that under conditions where ~90% of viral transcript abundance was reduced, the expression of only 241 of a total of 3,233 virally regulated genes was affected. These findings suggest that the intracellular signals generated in response to RSV

replication are maximally saturated at low viral loads. Of those RSV-controlled genes whose expression was reduced by ribavirin (Table 2), we found genes important in cell cycle progression and genes for cytokines, growth factors, receptors, signaling proteins, and transcription factors. Importantly, ribavirin had little effect on virus-induced chemokine expression. The effect of ribavirin on the expression of epithelial chemokines is pertinent because of their central role in coordinating airway inflammation. For example, our previous mRNA profiling studies have shown that RSV induces the expression of CC (I-309, Exodus-1, TARC, RANTES, MCP-1, MDC, MIP-1α, and MIP-1β), CXC (GRO-α, -β, and -γ; ENA-78; IL-8; and I-TAC), and CX_3C (Fractalkine) chemokines (67). In spite of producing an ~90% inhibition of viral transcription, ribavirin reduced the expression of only 2 of the 16 chemokines normally induced by RSV infection in these cells (67). These
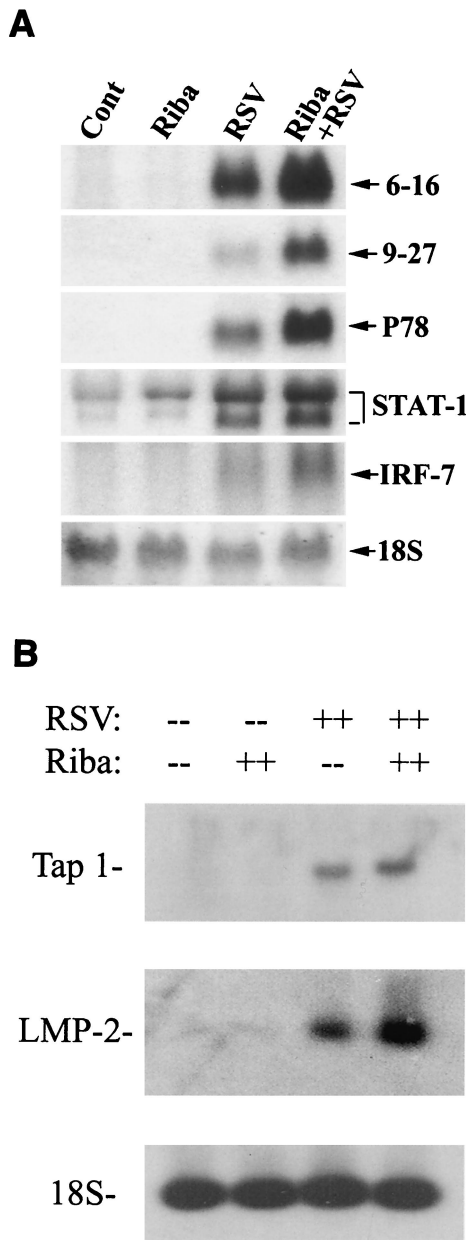
A

B

FIG. 5. Ribavirin's effect on the expression of TAP-1–LMP2 genes. (A) Potentiating effect of ribavirin on ISGs as shown by Northern blot analysis. Equal amounts of RNA samples (20 μg) from untreated control (Cont) and ribavirin (Riba)-, RSV-, or ribavirin- and RSV-treated (Riba + RSV) A549 cells were separated and hybridized with specific cDNA probes for IFI 6-16, IFI 9-27, MxA/p78, STAT-1, and IRF-7B; transcripts are indicated at right. The hybridization signal for 18S RNA is shown as the loading control. (B) Expression of the TAP-1–LMP2 locus. A549 cells were treated as described for Fig. 5A, and total RNA was isolated. Shown are the results of Northern blot hybridization for TAP-1 and LMP2 as indicated at right. The bottom panel shows the results of RNA hybridization for 18S RNA as a recovery marker.

chemokines, MIP-1α and -1β, are CC-type chemokines and are of particular relevance to RSV-induced immunopathology. A chemoattractant for B cells and cytotoxic T cells (51), MIP-1α is abundantly expressed by epithelial cells and can be

detected in alveoli, bronchioles, and adjacent capillary endothelium in a mouse model of RSV LRT infection (30). MIP-1α appears to play an important role in lung pathology, as MIP-1α-deficient mice have significantly reduced cellular inflammation following RSV infection (30). We note that MIP-1α and -1β were previously identified as having distinct expression profiles from those of the ribavirin-insensitive chemokines by their unique expression patterns in a bioinformatics analysis of RSV-inducible chemokine expression (67). These findings suggest that MIPs are controlled by a distinct ribavirin-sensitive regulatory pathway in RSV-infected cells. Moreover, that infected epithelial cells still strongly express the majority of chemokines after ribavirin treatment suggests to us that the epithelial chemokine response is triggered even by low levels of RSV replication. Practically, these findings imply to us that drugs aimed at reducing virus-induced inflammation in the lung may have to specifically target virus-induced signaling pathways rather than only inhibit viral transcription. Along these lines, an intriguing study suggested that a combination of antiviral and immunosuppressive agents was required to reduce pulmonary inflammation in a cotton rat model of RSV infection (where neither the antiviral nor the immunosuppressive treatment was beneficial alone) (50).

The ability of RSV to influence the expression of cell surface receptors may provide an important clue to the cellular biology of viral infection. Through this mechanism, a virally infected cell may have a cellular response distinct from that of its noninfected neighbor. Our functional analysis of the genes that were RSV inducible, but inhibited by ribavirin, highlighted a cell surface receptor group that included the PEG2 receptor, the adenosine A2 receptor, and the IL-2 receptor gamma chain (Table 2). Primary RSV infections result in a significant production of arachidonic acid metabolites, including PEG2 (24, 25); the fact that RSV also induces expression of the PGE2 receptor indicates that the virally infected cell may be highly responsive to locally generated PGE2, a ligand receptor pathway that induces the cyclic AMP second messenger and chloride secretion (41), alters ciliary beat frequency (33), or induces genetic responses via the CREB/ATF transcription factors (12). Similarly, RSV infection potentially induces a paracrine IL-15 response pathway. RSV induces not only the antiapoptotic cytokine IL-15 but also the IL-2 receptor γ chain, a component of the IL-15 receptor, suggesting that perhaps IL-15 has an as-yet-unknown paracrine action in RSV-infected epithelium. For both the PGE2 and IL-15 paracrine pathways, ribavirin reduces the expression of both the ligand and its receptor (Table 2). Finally, RSV is a potent inducer of adenosine A2 receptor expression, increasing its level by ~70-fold (Table 2). Activation of the adenosine A2 receptor in lung epithelial cells induces cyclic AMP accumulation and chloride secretion, perhaps inducing significant changes in the ionic composition of the extracellular lining fluid (41). In addition, the major site for pulmonary surfactant secretion, type II pneumocytes, responds to adenosine A2 receptor activation through enhanced phosphatidylcholine secretion (28). The mechanism for enhanced phosphatidylcholine secretion is not known to us but may be protective to maintain surface tension in the setting of LRT infection. A series of clinical observations have indicated that surfactant phospholipids are reduced in severe RSV LRT infection and that the exogenous adminis-
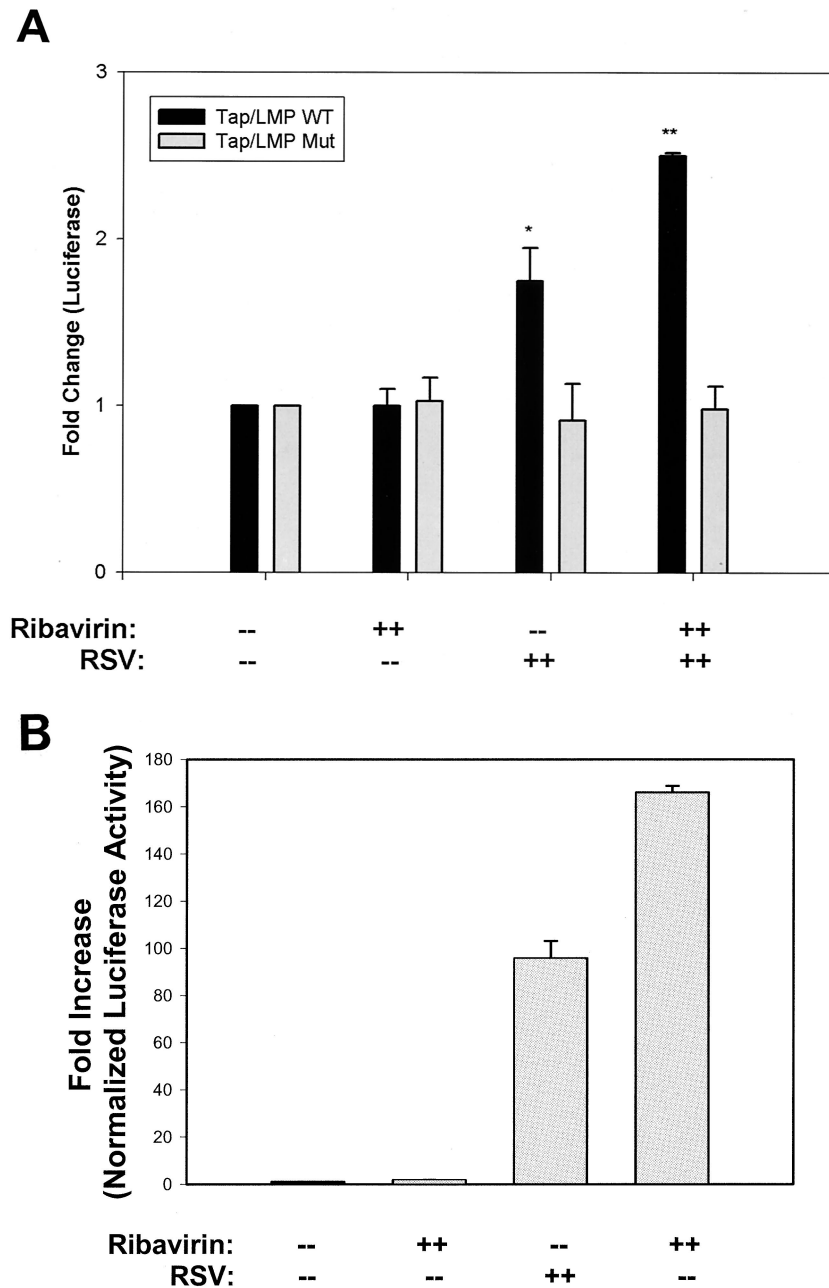
FIG. 6. Ribavirin treatment potentiates RSV-induced TAP-1–LMP2 transcriptional activity. (A) A549 cells transiently transfected with either pWT.LMP2-TAP-1.Luc (WT) or pMut.ISRE.Luc (Mut). Following transfection, cells were pretreated with ribavirin (100 µg/ml) for 2 h or not treated and infected with RSV (MOI, 1) for 15 h or not treated. Luciferase activity was normalized to β-Gal and expressed as the multiple of the level of induction over that of the control (uninfected). ∗, $P < 0.001$ compared to results with RSV alone. (B) Cells were transfected with the multimeric ISRE Luc reporter plasmid. Treatment and assay were as described for panel A.

tration of surfactant may produce a more rapid improvement in oxygenation and ventilation indices (60). Because ribavirin reduces adenosine A2 receptor expression, it may reduce the lung's ability to compensate for surfactant depletion in LRT infection.

The effect of ribavirin to further up-regulate the virus-induced expression of ISGs with potent antiviral functions (group II in Fig. 3b and Table 3) was of significant interest to us. This finding suggests that ribavirin interferes with a nega-

tive regulatory signal in the IFN pathway. IFN-β, the only IFN produced by RSV infection in vitro, is a highly inducible cytokine that is important in the innate mucosal response to virus (52). The liganded IFN-β receptor activates the STAT-1 and -2 transcription factors by tyrosine phosphorylation; these, in turn, associate with p48, producing the ISGF3 complex that enters the nucleus to induce gene expression (56). In RSV-infected epithelial cells, the actions of IFN-β partially mediate MHC class I up-regulation by inducing expression of the TAP-

FIG. 7. Enhanced binding of STAT-1 to the TAP-1–LMP2 ISRE. Biotinylated DNA (corresponding to the TAP-1–LMP2 ISRE site) was used to pull down nuclear proteins from control (Cont), ribavirin-treated (Riba), RSV-infected (RSV), or RSV- and ribavirin-treated (Riba + RSV) cells as described for Fig. 4B. Shown is a Western blot of the affinity-isolated proteins stained with antibody to STAT-1. Ribavirin increases the binding of STAT-1α and -1β to the ISRE compared to that induced by RSV infection alone.

1–LMP2/LMP7 locus (39) and have been shown to confer resistance to viral infection through ISG expression of protein kinase R, 2′-5′ oligoadenylate synthetases, and the p56 and MxA/p78 proteins (52, 56). In this study, we have shown the surprising findings that ribavirin potentiates the expression of MxA/p78 and the p56 genes. MxA/p78 is a cytoplasmic GTPase that has potent antiviral activities (reference 3 and references therein). In A549 cells, RSV increases the expression of MxA/p78 by ~200-fold; ribavirin further up-regulates this expression by ~350-fold (Fig. 5; Table 2). Although RSV is specifically resistant to the antiviral actions of MxA, the induction of MxA may potentiate the antiviral effects of ribavirin for a number of other negative-strand RNA viruses sensitive to its action, including influenza virus, vesicular stomatitis virus, measles virus, and parainfluenza virus (3). Similarly, p56 is a highly inducible cytoplasmic protein containing a tetratricopeptide domain that mediates specific protein interactions with elongation-initiation factor 3, blocking the initiation of cellular protein synthesis in virally infected cells. In the presence of viral replication, p56 is up-regulated by ~390-fold; in the presence of ribavirin, this up-regulation is increased to ~670-fold (Table 2). Together, these findings indicate that ribavirin potentiates the expression of antiviral ISGs.

Because ribavirin treatment reduces IFN-β expression, the further up-regulation of the ISGs was striking. We recognize that our studies do not prove that ribavirin up-regulates the IFN signaling pathway because ISG expression can also be induced by the production of double-stranded RNA independently of IFN production (52). However, since the viral RNA load is reduced as a function of ribavirin treatment, we suggest that ISG up-regulation is not due to an enhanced double-stranded RNA signaling pathway. Our preliminary studies suggest that ribavirin up-regulates ISRE action through a mechanism that partly involves enhanced STAT-1 DNA binding (Fig. 7). Enhanced STAT-1 binding may be the consequence of an enhanced STAT-1 synthetic rate (Table 3), enhanced STAT-1 tyrosine phosphorylation, or an indirect effect caused by reducing the expression of upstream STAT inhibitors (such as STAT inhibitor 2 [Table 2]). Of relevance here, others have shown that a complex of nonphosphorylated STAT-1 and IRF1 binds and enhances expression of the TAP-1–LMP2 ISRE (14), suggesting that enhanced STAT-1 tyrosine phosphorylation is not necessary for the activation of a subset of ISREs. Recently, the RSV nonstructural (NS) proteins NS1 and NS2 have been shown to antagonize the antiviral actions of IFN (7);

it is possible that ribavirin's effect of reducing NS protein production may be relevant to ISRE pathway activation. Further studies will be needed to resolve these relationships. Finally, we cannot account for all of the transcriptional induction of the ISRE by the weak changes in STAT-1 binding, and indeed in preliminary data not shown, we have also seen enhanced IRF7 binding to the TAP-1–LMP2 ISRE. The synthesis of IRF-7 is totally dependent on IFN-β signaling, and its expression appears to be important in the late induction of type I IFN-responsive genes (44). IRF-7 is activated during viral infection and becomes a major component in complexes binding ISREs in the 6-16 (49), TAP-1–LMP2, and other promoters (44, 57, 64). The potentiation of STAT- and IRF-dependent transcription further suggests that ribavirin-treated RSV-infected cells have distinct intracellular signaling programs.

Our study adds new mechanistic information on the close relationship between type I IFN effects and clinical response to ribavirin treatment that may be of significance in the treatment of other chronic viral infections. For example, in patients chronically infected with hepatitis C virus, ribavirin is used as an adjunct treatment for those who fail to respond to IFN-α alone (17, 18). We propose that ribavirin may act as an IFN-sensitizing agent, making virus-infected cells more responsive to IFN through ribavirin's ability to activate ISRE-dependent signaling.

In conclusion, ribavirin has multiple effects on cellular pathways in the setting of RSV infection. Although ribavirin reduces virus-induced expression of the CC chemokines MIP-1α and MIP-1β, an important finding is that epithelial cells still have a largely intact genomic inflammatory response program. These findings suggest that epithelial-cell signaling pathways controlling chemokine expression are potently activated by low levels of viral replication. We suggest that antiviral agents may be more efficacious in blocking airway inflammation when they are combined with inhibitors of intracellular signaling pathways controlling chemokine expression. Moreover, the actions of ribavirin to up-regulate the ISRE-signaling pathway and ISG expression may provide mechanistic insight into an additional mechanism for antiviral action.

REFERENCES

1. **Adler, K. B., B. M. Fischer, D. T. Wright, L. A. Cohn, and S. Becker.** 1994. Interactions between respiratory epithelial cells and cytokines: relationships to lung inflammation. Ann. N. Y. Acad. Sci. **725:**128–145.
2. **Aherne, W. T., T. Bird, S. D. B. Court, P. S. Gardner, and J. McQuillin.** 1970. Pathological changes in virus infections of the lower respiratory tract in children. J. Clin. Pathol. **23:**7–18.
3. **Atreya, P. L., and S. Kulkarni.** 1999. Respiratory syncytial virus strain A2 is resistant to the antiviral effects of type I interferons and human MxA. Virology **261:**227–241.
4. **Barnes, P. J., and M. Karin.** 1997. Nuclear factor-kappaB: a pivotal transcription factor in chronic inflammatory diseases. N. Engl. J. Med. **336:**1066–1071.

5. **Becker, S., W. Reed, F. W. Henderson, and T. L. Noah.** 1997. RSV infection of human airway epithelial cells causes production of the β-chemokine RANTES. Am. J. Physiol. **272:**L512–L520.

6. **Bennett, C. R., Jr., and D. Hamre.** 1962. Growth and serological characteristics of respiratory syncytial virus. J. Infect. Dis **110:** 8–16.

7. **Bossert, B., and K.-K. Conzelmann.** 2002. Respiratory syncytial virus (RSV) nonstructural (NS) proteins as host range determinants: a chimeric bovine RSV with NS genes from human RSV is attenuated in interferon-competent bovine cells. J. Virol. **76:**4287–4293.

8. **Brasier, A. R., M. Jamaluddin, A. Casola, W. Duan, Q. Shen, and R. Garofalo.** 1998. A promoter recruitment mechanism for TNF-α-induced IL-8 transcription in type II pulmonary epithelial cells: dependence on nuclear abundance of Rel A, NF-κB1, and c-Rel transcription factors. J. Biol. Chem. **273:**3551–3561.

9. **Brasier, A. R., J. E. Tate, and J. F. Habener.** 1989. Optimized use of the firefly luciferase assay as a reporter gene in mammalian cell lines. BioTechniques **7:**1116–1122.

10. **Casola, A., N. Burger, T. Liu, M. Jamaluddin, A. R. Brasier, and R. P. Garofalo.** 2001. Oxidant tone regulates RANTES gene expression in airway epithelial cells infected with RSV. J. Biol. Chem. **276:**19715–19722.

11. **Casola, A., R. Garofalo, M. Jamaluddin, S. Vlahopoulos, and A. R. Brasier.** 2000. Requirement of a novel upstream response element in respiratory syncytial virus-induced IL-8 gene expression. J. Immunol. **164:**5944–5951.

12. **Casola, A., R. P. Garofalo, H. Haeberle, T. Elliott, R. Lin, M. Jamaluddin, and A. R. Brasier.** 2001. Multiple cis regulatory elements control RANTES promoter activity in alveolar epithelial cells infected with respiratory syncytial virus. J. Virol. **75:**6428–6439.

13. **Chatterjee-Kishore, M., R. Kishore, D. J. Hicklin, F. M. Marincola, and S. Ferrone.** 1998. Different requirements for signal transducer and activator of transcription 1 alpha and interferon regulatory factor 1 in the regulation of low molecular mass polypeptide 2 and transporter associated with antigen processing 1 gene expression. J. Biol. Chem. **273:**16177–16183.

14. **Chatterjee-Kishore, M., K. L. Wright, J. P. Ting, and G. R. Stark.** 2000. How Stat1 mediates constitutive gene expression: a complex of unphosphorylated Stat1 and IRF1 supports transcription of the LMP2 gene. EMBO J. **19:**4111–4122.

15. **Committee on Infectious Diseases.** 1993. Use of ribavirin in the treatment of respiratory syncytial virus in infection. Pediatrics **92:**501–504.

16. **Crotty, S., C. E. Cameron, and R. Andino.** 2001. RNA virus error catastrophe: direct molecular test by using ribavirin. Proc. Natl. Acad. Sci. USA **98:**6895–6900.

17. **Di Bisceglie, A. M., J. Thompson, N. Smith-Wilkaitis, E. M. Brunt, and B. R. Bacon.** 2001. Combination of interferon and ribavirin in chronic hepatitis C: re-treatment of nonresponders to interferon. Hepatology **33:**704–707.

18. **Ferenci, P., R. Stauber, P. Steindl-Munda, M. Gschwantler, P. Fickert, C. Datz, C. Muller, F. Hackl, W. Rainer, T. Watkins-Riedel, W. Lin, G. J. Krejs, A. Gangl, and the Austrian Hepatitis Study Group.** 2001. Treatment of patients with chronic hepatitis C not responding to interferon with high-dose interferon alpha with or without ribavirin: final results of a prospective randomized trial. Hepatology **13:**699–705.

19. **Ferris, J. A., W. A. Aherne, and W. S. Locke.** 1973. Sudden and unexpected deaths to infants: histology and virology. Br. Med. J. **2:**439–449.

20. **Fiedler, M. A., K. Wernke-Dollries, and J. M. Stark.** 1995. Respiratory syncytial virus increases IL-8 gene expression and protein release in A549 cells. Am. J. Physiol. **269:**L865–L872.

21. **Fiedler, M. A., K. Wernke-Dollries, and J. M. Stark.** 1996. Inhibition of viral replication reverses respiratory syncytial virus-induced NF-κB activation and interleukin-8 gene expression in A549 cells. J. Virol. **70:**9079–9082.

22. **Garenne, M., C. Ronsmans, and H. Campbell.** 1992. The magnitude of mortality from acute respiratory infections in children under 5 years in developing countries. World Health Stat. Q. **45:**180–191.

23. **Garofalo, R., M. Sabry, M. Jamaluddin, R. K. Yu, A. Casola, P. L. Ogra, and A. R. Brasier.** 1996. Transcriptional activation of the interleukin-8 gene by respiratory syncytial virus infection in alveolar epithelial cells: nuclear translocation of the RelA transcription factor as a mechanism producing airway mucosal inflammation. J. Virol. **70:**8773–8781.

24. **Garofalo, R., R. C. Welliver, and P. L. Ogra.** 1991. Concentrations of LTB4, LTC4, LTD4 and LTE4 in bronchiolitis due to respiratory syncytial virus. Pediatr. Allergy Immunol. **2:**30–37.

25. **Gershwin, L., S. N. Girid, R. S. Stewart, and J. Chen.** 1989. Prostaglandin and thromboxane concentrations in plasma and lung lavage fluids during sequential infection of vaccinated and nonvaccinated calves with bovine respiratory syncytial virus. Am. J. Vet. Res. **50:**1254–1262.

26. **Gilbert, B. E., and V. Knight.** 1986. Biochemistry and clinical applications of ribavirin. Antimicrob. Agents Chemother. **30:**201–205.

27. **Glezen, W. P., L. H. Taber, and A. L. Frank.** 1986. Risk of primary infection and reinfection with respiratory syncytial virus. Am. J. Dis. Child. **140:**543–546.

28. **Griese, M., L. I. Gobran, J. S. Douglas, and S. A. Rooney.** 1991. Adenosine A2-receptor-mediated phosphatidylcholine secretion in type II pneumocytes. Am. J. Physiol. **260:**L52–L60.

29. **Grosfeld, H., M. G. Hill, and P. L. Collins.** 1995. RNA replication by respiratory syncytial virus (RSV) is directed by the N, P, and L proteins; transcription also occurs under these conditions but requires RSV superinfection for efficient synthesis of full-length mRNA. J. Virol. **69:**5677–5686.

30. **Haeberle, H. A., W. A. Kuziel, H.-J. Dieterich, A. Casola, Z. Gatalica, and R. P. Garofalo.** 2001. Inducible expression of inflammatory chemokines in respiratory syncytial virus-infected mice: role of MIP-1α in lung pathology. J. Virol. **75:**878–890.

31. **Hall, C. B.** 2001. Respiratory syncytial virus and parainfluenza virus. N. Engl. J. Med. **344:**1917–1928.

32. **Hall, C. B., and C. A. McCarthy.** 1995. Respiratory syncytial virus, p. 1501. In G. L. Mandel, J. E. Bennett, and R. Dolin (ed.), Principles and practice of infectious diseases. Churchill Livingston, New York, N.Y.

33. **Hermoso, M., N. Barrera, B. Morales, S. Perez, and M. Villalon.** 2001. Platelet activating factor increases ciliary activity in the hamster oviduct through epithelial production of prostaglandin E2. Eur. J. Physiol. **442:**336–345.

34. **Horisberger, M. A., G. K. McMaster, H. Zeller, M. G. Wathelet, J. Dellis, and J. Content.** 1990. Cloning and sequence analyses of cDNAs for interferon- and virus-induced human Mx proteins reveal that they contain putative guanine nucleotide-binding sites: functional study of the corresponding gene promoter. J. Virol. **64:**1171–1181.

35. **Hruska, J. F., J. M. Bernstein, R. G. Douglas, Jr., and C. B. Hall.** 1980. Effects of ribavirin on respiratory syncytial virus in vitro. Antimicrob. Agents Chemother. **17:**770–775.

36. **Jamaluddin, M., A. Casola, R. P. Garofalo, Y. Han, T. Elliott, P. L. Ogra, and A. R. Brasier.** 1998. The major component of IκBα proteolysis occurs independently of the proteasome pathway in respiratory syncytial virus-infected pulmonary epithelial cells. J. Virol. **72:**4849–4857.

37. **Jamaluddin, M., R. Garofalo, P. L. Ogra, and A. R. Brasier.** 1996. Inducible translational regulation of the NF-IL6 transcription factor by respiratory syncytial virus infection in pulmonary epithelial cells. J. Virol. **70:**1554–1563.

38. **Jamaluddin, M., T. Meng, J. Sun, I. Boldogh, Y. Han, and A. R. Brasier.** 2000. Angiotensin II induces nuclear factor (NF)-kappaB1 isoforms to bind the angiotensinogen gene acute-phase response element: a stimulus-specific pathway for NF-kappaB activation. Mol. Endocrinol. **14:**99–113.

39. **Jamaluddin, M., S. Wang, R. Garofalo, T. Elliott, A. Casola, S. Baron, and A. R. Brasier.** 2001. IFN-β mediates coordinate expression of antigen-processing genes in RSV-infected pulmonary epithelial cells. Am. J. Physiol. Lung Cell. Mol. Physiol. **280:** L248–L257.

40. **Jiang, Z., M. Kunimoto, and J. A. Patel.** 1998. Autocrine regulation and experimental modulation of interleukin-6 expression by human pulmonary epithelial cells infected with respiratory syncytial virus. J. Virol. **72:**2496–2499.

41. **Lazarowski, E. R., S. J. Mason, L. Clarke, T. K. Harden, and R. C. Boucher.** 1992. Adenosine receptors on human airway epithelia and their relationship to chloride secretion. Br. J. Pharmacol. **106:**774–782.

42. **Long, C. E., J. T. McBride, and C. B. Hall.** 1995. Sequelae of respiratory syncytial virus infections: a role for intervention studies. Am. J. Respir. Crit. Care Med. **151:**1678–1681.

43. **MacDonald, N. E., C. B. Hall, and S. C. Suffin.** 1982. Respiratory syncytial viral infection in infants with congenital heart disease. N. Engl. J. Med. **307:**397–400.

44. **Marie, I., J. E. Durbin, and D. Levy.** 1998. Differential viral induction of distinct interferon-alpha genes by positive feedback through interferon regulatory factor-7. EMBO J. **17:**6660–6669.

45. **Martin, L. D., L. G. Rochelle, B. M. Fischer, T. M. Krunkosky, and K. B. Adler.** 1997. Airway epithelium as an effector of inflammation: molecular regulation of secondary mediators. Eur. Respir. J. **10:** 2139–2146.

46. **Min, W., J. S. Pober, and D. R. Johnson.** 1996. Kinetically coordinated induction of TAP1 and HLA class I by IFN-gamma: the rapid induction of TAP1 by IFN-gamma is mediated by Stat1 alpha. J. Immunol. **156:**3174–3183.

47. **Noah, T. L., and S. Becker.** 1993. Respiratory syncytial virus-induced cytokine production by a human bronchial epithelial cell line. Am. J. Physiol. **265:** L472–L478.

48. **Olzewska-Pazdrak, B., A. Casola, T. Saito, R. Alam, S. E. Crowe, F. Mei, P. L. Ogra, and R. P. Garofalo.** 1998. Cell-specific expression of RANTES, MCP-1, and MIP-1α by lower airway epithelial cells and eosinophils infected with respiratory syncytial virus. J. Virol. **72:**4756–4764.

49. **Porter, A. C., Y. Chernajovsky, T. C. Dale, C. S. Gilbert, G. R. Startk, and I. M. Kerr.** 1988. Interferon response element of the human gene 6–16. EMBO J. **7:**85–92.

50. **Prince, G. A., A. Mathews, S. J. Curtis, and D. D. Porter.** 2000. Treatment of respiratory syncytial virus bronchiolitis and pneumonia in a cotton rat model with systemically administered monoclonal antibody (palivizumab) and glucocorticosteroid. J. Infect. Dis. **182:** 1326–1330.

51. **Schall, T. J., K. Bacon, R. D. Camp, J. W. Kaspari, and D. V. Goeddel.** 1993. Human macrophage inflammatory protein alpha (MIP-1 alpha) and MIP-1 beta chemokines attract distinct populations of lymphocytes. J. Exp. Med. **177:**1821–1826.

52. **Sen, G. C.** 2001. Viruses and interferons. Annu. Rev. Microbiol. **55:**255–281.

53. **Shay, D. K., R. C. Holman, R. D. Newman, L. L. Liu, J. W. Stout, and L. J.**

Anderson. 1999. Bronchiolitis-associated hospitalizations among US children, 1980–1996. JAMA **282:**1440–1446.

54. **Shay, D. K., R. C. Holman, G. E. Roosevelt, M. J. Clarke, and L. J. Anderson.** 2001. Bronchiolitis-associated mortality and estimates of respiratory syncytial virus-associated deaths among US children, 1979–1997. J. Infect. Dis. **183:** 16–22.

55. **Sherman, C. T., and A. R. Brasier.** 2001. Role of STAT1 and STAT3 in inducible expression of the human angiotensinogen gene by interleukin-6. Mol. Endocrinol. **15:**441–457.

56. **Stark, G. R., I. M. Kerr, B. R. G. Williams, R. H. Silverman, and R. D. Schreiber.** 1998. How cells respond to interferons. Annu. Rev. Biochem. **67:**227–264.

57. **Taniguchi, T., K. Ogasawara, A. Takaoka, and N. Tanaka.** 2001. IRF family of transcription factors as regulators of host defense. Annu. Rev. Immunol. **19:**623–655.

58. **Thomas, L. H., J. S. Friedland, M. Sharland, and S. Becker.** 1998. Respiratory syncytial virus-induced RANTES production from human bronchial epithelial cells is dependent on nuclear factor-kappa B nuclear binding and is inhibited by adenovirus-mediated expression of inhibitor of kappa B alpha. J. Immunol. **161:**1007–1016.

59. **Tian, B., Y. Zhang, B. A. Luxon, R. P. Garofalo, A. Casola, M. Sinha, and A. R. Brasier.** 2002. Identification of NF-κB-dependent gene networks in respiratory syncytial virus-infected cells. J. Virol. **76:**6800–6814.

60. **Tibby, S. M., M. Hatherill, S. M. Wright, P. Wilson, A. D. Postle, and I. A. Murdoch.** 2000. Exogenous surfactant supplementation in infants with respiratory syncytial virus bronchiolitis. Am. J. Respir. Crit. Care Med. **162:** 1251–1256.

61. **Ueba, O.** 1978. Respiratory syncytial virus. I. concentration and purification of the infectious virus. Acta Med. Okayama **32:**265–272.

62. **Vastag, M., J. Skopal, J. Kramer, K. Kolev, Z. Voko, E. Csonka, R. Machovich, and Z. Nagy.** 1998. Endothelial cells cultured from human brain microvessels produce complement proteins factor H, factor B, C1 inhibitor, and C4. Immunobiology **199:**5–13.

63. **Wathelet, M. G., S. Moutschen, P. Defilippi, A. Cravador, M. Collet, G. Huez, and J. Content.** 1986. Molecule cloning, full length sequence and preliminary characterization of a 56 kDa protein induced by human interferons. Eur. J. Biochem. **155:**11–17.

64. **Wathelet, M. G., L. C. Ronco, P. M. Howley, and T. Maniatis.** 1998. Virus infection induces the assembly of coordinately activated transcription factors on the IFN-β enhancer in vivo. Mol. Cell **1:**507–518.

65. **Wyde, P. R.** 1998. Respiratory syncytial virus (RSV) disease and prospects for its control. Antivir. Res. **39:**63–79.

66. **Yu, Q., R. W. Hardy, and G. W. Wertz.** 1995. Functional cDNA clones of the human respiratory syncytial (RS) virus N, P, and L proteins support replication of RS virus genomic RNA analogs and define minimal *trans*-acting requirements for RNA replication. J. Virol. **69:**2412–2419.

67. **Zhang, Y., B. A. Luxon, A. Casola, R. P. Garofalo, M. Jamaluddin, and A. R. Brasier.** 2001. Expression of RSV-induced chemokine gene networks in lower airway epithelial cells revealed by cDNA microarrays. J. Virol. **75:** 9044–9058.